Friction

Research Article

Efficient wear resistance at the steel/steel friction interface achieved through Span65 confined PAO10 gel lubricant

Kunpeng Li[1,2], Liqiang Zhang[2,3,✉], Changhe Du[2,4], Runhao Zheng[3,4], Liucheng Wang[2,4], Shoukui Gao[1], Jian Zhang[2], Youqiang Wang[1,✉], Daoai Wang[3,✉]

Cite this article: Li KP, Zhang LQ, Du CH, et al. *Friction* 2026, **14**(1): 9441070. https://doi.org/10.26599/FRICT.2025.9441070

ABSTRACT: Ultra-low wear technology provides an effective solution to prolong the service life of mechanical equipment. However, there are still significant challenges in achieving ultra-low wear at the steel/steel interface over long periods. In this work, a PAO10-SPAN65 composite semisolid lubricant (PAO10/SP65) was designed with sorbitan tristearate (SPAN65) and base oil poly α-olefin 10 (PAO10). The wear rate of the steel lubricated with PAO10/SP65 (1.31×10^{-8} $mm^3\cdot N^{-1}\cdot m^{-1}$) was 96% lower than that of PAO10 (3.52×10^{-7} $mm^3\cdot N^{-1}\cdot m^{-1}$). In addition, after 10 h of friction testing at a contact pressure of 0.82 GPa, the wear of the steel surface is still close to zero, with a wear rate of 4.13×10^{-9} $mm^3\cdot N^{-1}\cdot m^{-1}$. This study provides a new design idea for realizing ultra-low wear of engineering steel.

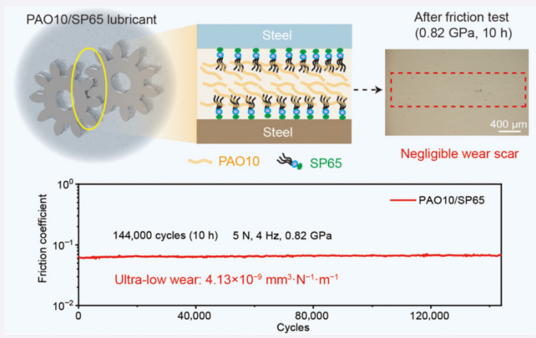

KEYWORDS: ultra-low wear; sorbitan tristearate; semisolid lubricant; steel-steel friction

1 Introduction

Friction and wear increase the surface roughness and operating resistance of mechanical equipment, resulting in a reduction in equipment accuracy, a shortened service life, and additional energy loss [1–3]. Friction moving parts of steel-steel pairs are widely used in mechanical engineering, and the effective avoidance of the wear of steel surfaces has received increasing attention [4, 5]. At present, the roughness and wear depth of the material surface after the friction test are believed to be approximately equal to the roughness and wear depth of the original surface of the material, which is an ultra-low wear state. However, how to achieve ultra-low wear of the steel-steel contact interface is a difficult problem.

Liquid lubricants such as lubricating oil and grease are usually added to the steel-steel friction interface to reduce wear. However, the lubrication performance of liquid lubricants is affected by factors such as lubricant components, rheological properties, and motion conditions [6–10]. Although the bearing ability of high-viscosity lubricants is excellent, the viscous resistance generated by friction and their poor fluidity may make it difficult to form a lubricating film that uniformly covers the metal surface in a short time, resulting in material wear. The lubricating film formed by low-viscosity lubricants with lower interface resistance may be destroyed under higher loads, resulting in wear of the material [11–13]. In addition, the speed of movement and viscosity affect the lubrication performance of lubricants, which are affected by the pressure of the lubricating oil at the interface and the wettability of the friction surface [14–16]. At present, several new liquid lubricants, such as acid aqueous solutions [17, 18], polyol solutions [19–21], and ionic liquids [22, 23], have been applied for lubrication at the steel-steel interface. Although they exhibit excellent superlubrication properties, ionic liquids and polyol solutions have a long run-in period during friction, which causes wear on the surface of the material. An acidic-aqueous solution may have problems such as lubrication failure and corrosion wear in the process of long-term friction. Du et al. [24] used polyethylene glycol, citric acid, and carbon quantum dots to make the liquid lubricant shorten the run-in time and achieve ultra-low wear during steel-steel interface friction. However, the water-based lubricant may volatilize during a longer friction process, making it difficult to continue lubrication. Therefore, it is vitally important to develop a new lubricant with significant wear resistance performance at the steel–steel interface.

In this work, a PAO10-SPAN65 composite semisolid lubricant (PAO10/SP65) was prepared with sorbitan tristearate (SPAN65) as an additive and base oil poly α-olefin (PAO10). The lubrication performance of PAO10/SP65 was evaluated in linear reciprocating mode via a ball-and-disc friction machine. The results show that PAO10/SP65 has almost no running-in period during friction and

[1] School of Mechanical and Automotive Engineering, Qingdao University of Technology, Qingdao 266525, China. [2] Shandong Laboratory of Advanced Materials and Green Manufacturing at Yantai, Yantai 264000, China. [3] State Key Laboratory of Solid Lubrication, Lanzhou Institute of Chemical Physics, Chinese Academy of Sciences, Lanzhou 730000, China. [4] Qingdao Center of Resource Chemistry and New Materials, Qingdao 266104, China.

✉ Corresponding authors. E-mail: L. Zhang, zhangliqiang@licp.cas.cn; Y. Wang, wyq1970301@126.com; D. Wang, wangda@licp.cas.cn

Received: November 8, 2024; Revised: December 19, 2024; Accepted: January 22, 2025

a wear volume reduction of approximately 25 times in comparison to PAO10. In addition, PAO10/SP65 can achieve ultra-low wear at the steel–steel friction interface even during a long (10 h) friction experiment. This work provides a new design idea for realizing ultra-low wear of engineering steel–steel contact interfaces and a new way to reduce the energy loss of mechanical devices.

2 Experimental

2.1 Materials

Shanghai Macklin Biochemical Technology Co., Ltd., China, provided the sorbitan tristearate (SPAN65). Shenzhen Huameite Lubrication Technology Co., Ltd., China, provided the base oil PAO10. The 9GCr18 steel block was purchased from Suzhou Feiyue Precision Machinery Co., Ltd., China. The steel balls (100CR6 and 440C, diameter: 9.5 mm, roughness (R_a): 25 nm) and ceramic balls (Si_3N_4 and ZrO_2, diameter: 9.5 mm, R_a: 25 nm) were purchased from Yiwu Hongzhou Trading Co., Ltd., China. All friction pairs were cleaned with absolute ethanol and petroleum ether before the friction test.

2.2 Tribological experiments

A friction machine (TRB3, Anton Paar, Austria) with a ball-on-disc mode was used for linear reciprocating friction experiments. The range of the applied load applied by the friction test is 1–20 N, the linear moving distance is 4 mm, and the frequency is 1–5 Hz.

2.3 Characterization after the friction test

A Fourier transform infrared spectroscope (FT-IR; PerkinElmer, Frontier, USA) was used to analyze the composition of the lubricant. The rheological properties of PAO10/SP65 were measured via a rheometer (MCR302, Anton Paar, Germany). A SINDIN optical contact angle measuring instrument was used to measure the contact angle (CA) of the base oil and PAO10/SP65 on the steel surface. The wear marks were analyzed via a microscope (Axioscope 5, Zeiss, Germany) and SEM (EVO-10, Zeiss, Germany). The wear area of each steel ball was analyzed via an X-ray photoelectron spectroscope (XPS; PHI5000 VersaprobeIII, ULVAC-PHI.INC, Japan). A noncontact optical 3D profiler (MicroXAM-800; KLA-Tencor, USA) was used to analyze the wear area of the steel block.

3 Results

3.1 Synthesis and analysis of PAO10/SP65

After physical heating and mixing, PAO10 and SP65 formed a uniform random network. After cooling, PAO10 is confined to the network of SP65 because of the low freezing point of SP65. After the solution completely cooled, the semisolid lubricant PAO10/SP65 was obtained, as illustrated in Fig. 1(a). FT-IR was used to characterize PAO10, SPAN65, and PAO10/SP65. The absorption peak observed at 1,741 cm^{-1} corresponds to the C=O bond. In addition, for PAO10/SP65, the O–H absorption peak of the original SPAN65 shifted from 3,492 to 3,458 cm^{-1}, as illustrated in Fig. 1(b). This phenomenon may be attributed to the alteration of the molecular filling pattern of SPAN65 by PAO10 through van der Waals forces. This interaction weakens the originally strong hydrogen bonds within or between molecules, leading to a decrease in the wavenumber associated with hydroxyl stretching vibrations.

In addition, the climbing behavior of PAO10 and PAO10/SP65 on the steel surface was observed. After 24 h, PAO10 clearly crawled. On the other hand, PAO10/SP65 exhibited excellent anti-creep performance on both vertical and horizontal steel blocks (Fig. 1(c) and Fig. S1 in the Electronic Supplementary Material (ESM)). This may be because the presence of hydroxyl groups enhances the adsorbability of the lubricant onto the material's surface [25].

3.2 Ultra-low wear behavior of PAO10/SP65

A friction machine was used to evaluate the frictional properties of the lubricant (Fig. 2(a)). Figure 2(b) and Fig. S2 in the ESM show

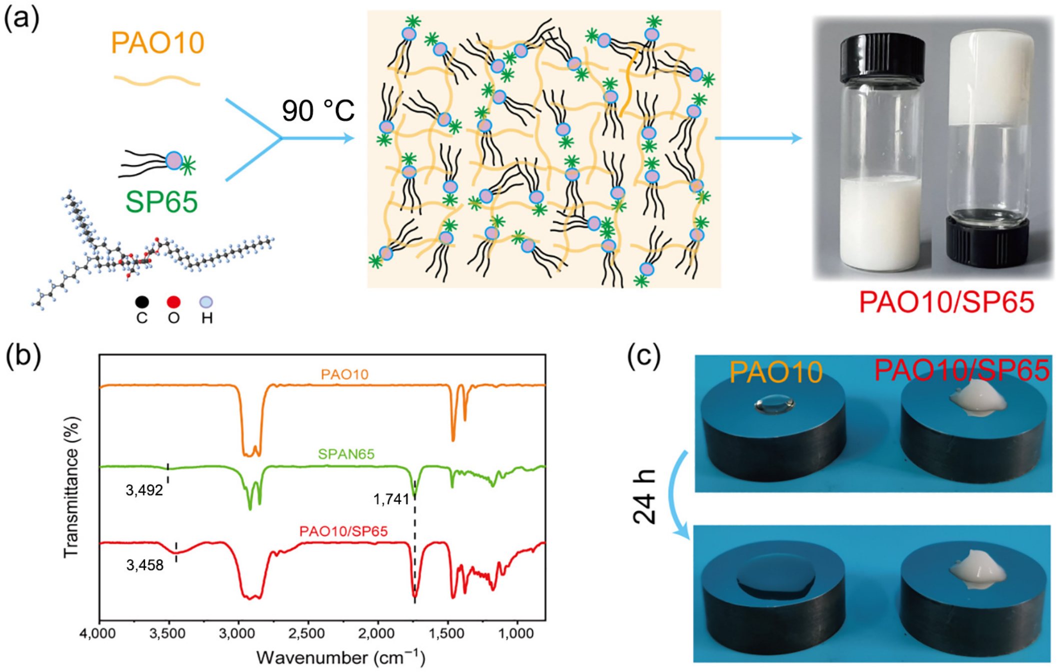

Fig. 1 (a) Synthesis diagram of PAO10/SP65. (b) Infrared spectra of PAO10, SPAN65, and PAO10/SP65. (c) Climbing diagram of PAO10 and PAO10/SP65 on the steel block surface.

the coefficient of friction (COF) curves for the three lubrication modes under a load of 5 N. The COF of the dry friction mode is approximately 0.7 because the metal surface is in direct contact without the intervention of lubricants, resulting in a large COF. Moreover, during the friction process, owing to plastic deformation, severe adhesion and violent wear of the metal surface, many microscopic bulges occur in the contact area, which leads to friction vibration and sharp fluctuations in the COF [26–30]. When the base oil PAO10 was introduced into the steel–steel friction interface, the COF was reduced to approximately 0.08. This occurs because of the formation of an oil film by the lubricating oil between the two contact surfaces, which diminishes the contact of the friction pair and consequently reduces frictional resistance. When PAO10/SP65 lubrication was used, the COF was approximately 0.05. A three-dimensional (3D) profiler characterized the wear area of the steel block. As illustrated in Fig. 2(c) and Fig. S3 in the ESM, dry friction has the highest wear rate, reaching ~8.41×10^{-6} $mm^3 \cdot N^{-1} \cdot m^{-1}$. When PAO10 lubrication is used, steel-steel wear is reduced to ~3.52×10^{-7} $mm^3 \cdot N^{-1} \cdot m^{-1}$. When PAO10/SP65 lubrication is utilized, the wear between steel and steel is notably diminished, resulting in a wear rate of approximately 1.31×10^{-8} $mm^3 \cdot N^{-1} \cdot m^{-1}$. Specifically, the wear rate of PAO10/SP65 was 96% lower than that of PAO10.

In addition, the 3D morphology of the three samples revealed that under the dry friction and PAO10 lubrication modes, the steel blocks had obvious wear marks (Figs. 2(d) and 2(e)), and the depths were 7 and 0.18 μm, respectively (Figs. 2(g) and 2(h)). In contrast, a steel block lubricated by PAO10/SP65 has negligible wear marks (Fig. 2(f)) and a depth close to zero (Fig. 2(i)). The experimental results show that PAO10/SP65 has excellent wear resistance.

The wear areas of the steel blocks and steel balls were examined via optical microscopy and scanning electron microscopy (SEM). These findings further validated the advantageous antiwear properties of the lubricant employed. The wear observed on the dry friction steel block is significant, with a wear mark width of 926.5 μm (Fig. 3(a)). When PAO10 was used as a lubricant, the width of the wear marks decreased to 141.3 μm (Fig. 3(b)). In contrast, the number of wear marks on the steel blocks lubricated with PAO10/SP65 is negligible (Fig. 3(c)). SEM was used to magnify the wear mark area further. In the state of dry friction, there are pits and a large amount of debris in the wear area (Fig. 3(d)). This is because the friction interface is in direct contact, which is prone to adhesive wear and abrasive wear, causing the microscopic particles on the metal surface to fall off, thus producing significant cutting effects on the material surface in relative motion, resulting in apparent grooves and pits in the wear area [31–34]. Under PAO10 lubrication conditions,

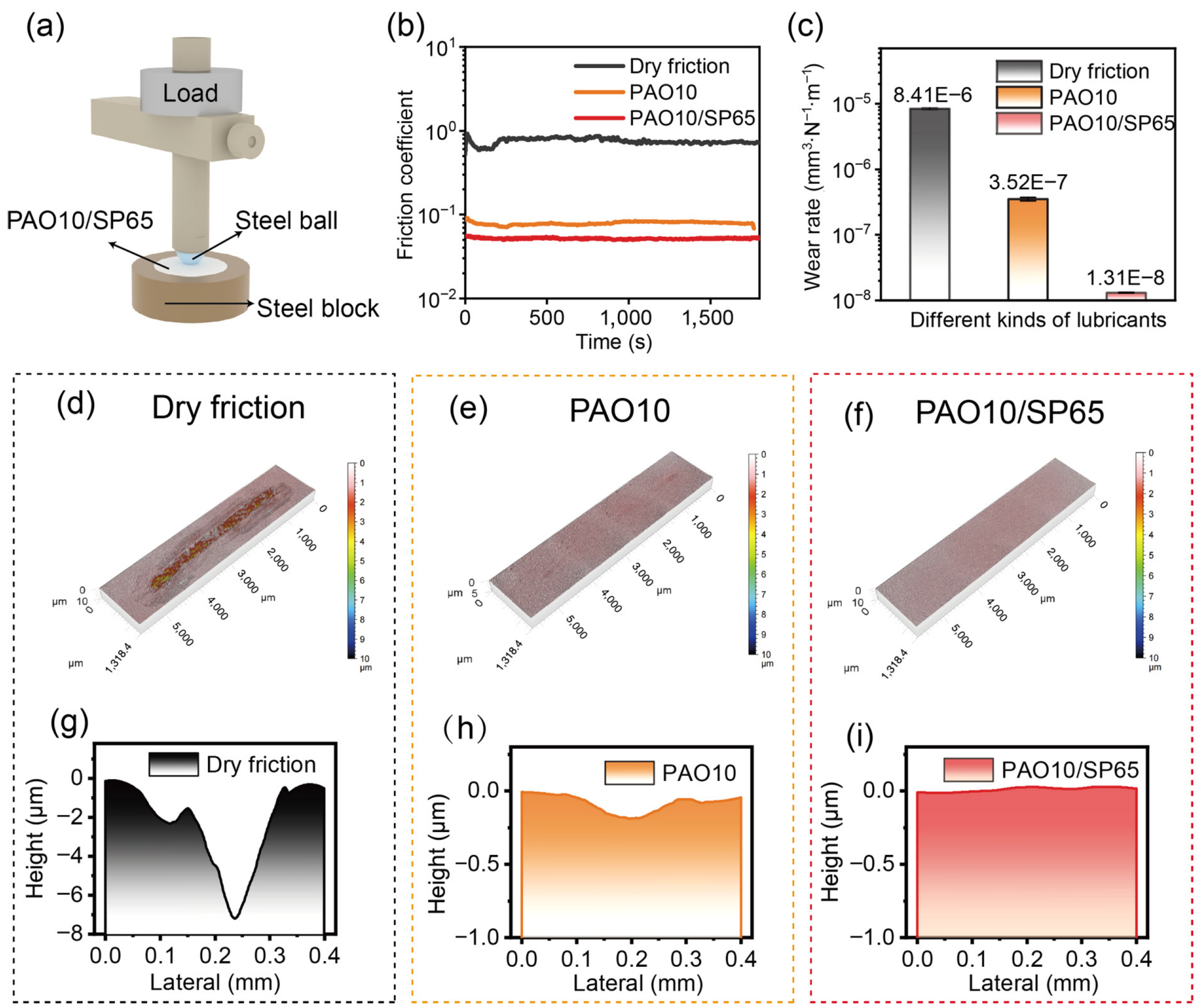

Fig. 2 (a) Friction test device diagram. (b) Friction coefficient curves for dry friction, PAO10, and PAO10/SP65. (c) Dry friction, with PAO10 and PAO10/SP65 as lubrication, and the wear rates of the steel blocks. (d–f) 3D profiles of the three lubrication modes. (g–i) Wear depths of the three lubrication modes. The test load was 5 N, the frequency was 4 Hz, and the test time was 1,800 s.

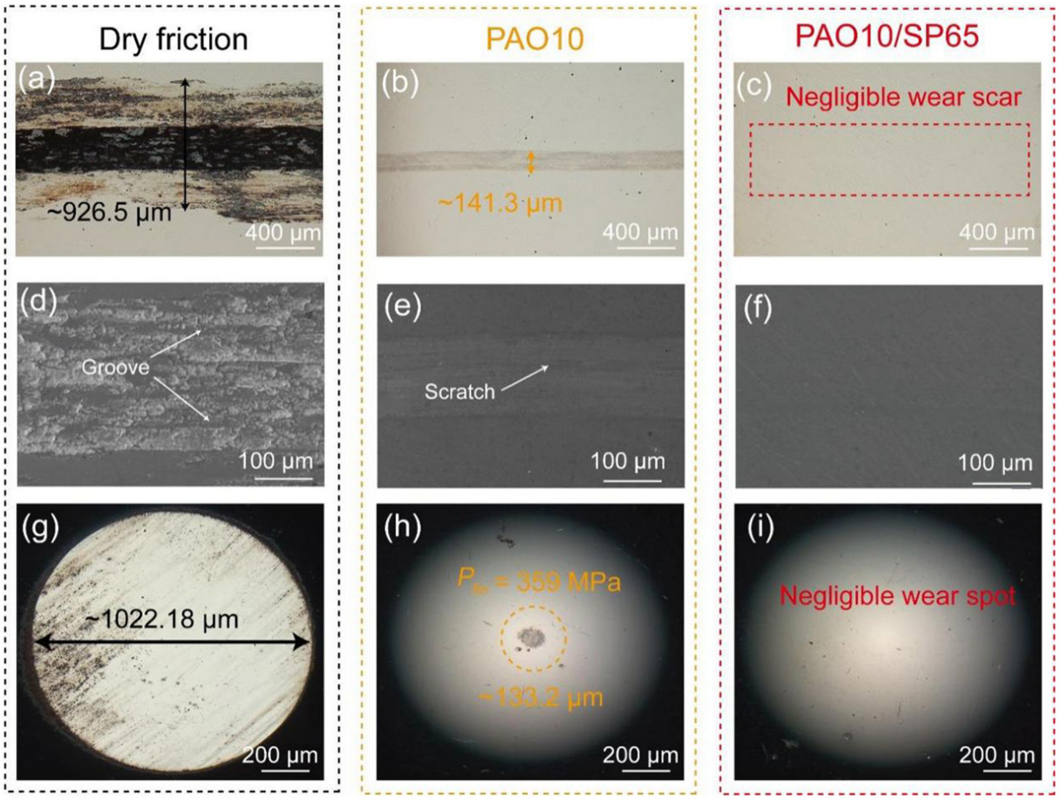

Fig. 3 (a–c) Optical photographs of the wear area under three lubrication modes (dry friction, PAO10, and PAO10/SP65). (d–f) SEM images of the wear area under the three lubrication modes. (g–i) Optical photographs of ball wear in the three lubrication modes.

scratches were still clearly observed in the area of the wear marks (Fig. 3(e)). This may be because the bearing capacity and adhesion of PAO10 are weak, and the oil film breaks during friction, thus making the steel-steel surface contact directly, resulting in wear. However, under PAO10/SP65 lubrication, wear was negligible in the corresponding SEM images (Fig. 3(f)). In addition, the diameter of the wear point on the steel ball subjected to dry friction was 1,022.18 μm (Fig. 3(g)). Under PAO10 lubrication, the diameter of the wear point on the steel ball was 133.2 μm (Fig. 3(h)). However, the wear point on the steel ball under PAO10/SP65 lubrication was negligible (Fig. 3(i)).

In addition, the actual contact pressure (P_{fin}) of base oil PAO10 was calculated to be 359 MPa on the basis of the ratio of the load area to the abrasion area. However, the measured contact pressure (P_{fin}) of the PAO10/SP65 lubricating friction pair is approximately equal to the initial pressure of 0.82 GPa. This observation indicates that the inclusion of SPAN65 significantly enhances the load-bearing capacity of the lubricating oil.

3.3 Effects of SPAN65 content on lubrication properties

To further enhance the wear resistance of lubricating oil, an analysis was conducted to investigate the effect of the SPAN65 content in PAO10/SP65 on lubrication performance (Fig. 4). Four ratios were selected for the tribological performance tests. As illustrated in Fig. 4(a), when the concentration of SPAN65 is maintained between 5 and 20 wt%, the COF ranges from approximately 0.06 to 0.08. When the content of SPAN65 reached 30 wt%, the COF decreased to approximately 0.05. The wear rate of the steel block at the specified wear area was measured via a 3D profiler. As illustrated in Fig. 4(b), the wear rate is lowest when the SPAN65 content reaches 30 wt%. The wear area was analyzed via optical microscopy and SEM, and the differences in the antiwear properties among the four ratios were further clarified. When PAO10/SP65 is lubricated with SPAN65 contents of 5 and 10 wt%, there are obvious wear marks on the steel blocks with widths of 148.8 and 144.3 μm, respectively, as shown in (i) and (ii) in Figs. 4(c) and 4(d). When the SPAN65 content in PAO10/SP65 is 20 wt%, the steel block only shows slight wear, and the wear width decreases to 116.9 μm, as shown in Figs. 4(e)(i) and 4(e)(ii). When the SPAN65 content reaches 30 wt%, the wear marks on the steel block are almost invisible, as shown in Figs. 4(f)(i) and 4(f)(ii). This occurred because the addition of SPAN65 increases the bearing capacity of the lubricant. Moreover, we found that the lubrication performance decreased when the proportion of SP65 was 40 wt%, which can be attributed to the increased viscosity of the lubricant as the proportion of SP65 increased. In addition, the lubricant is pushed to both sides during the friction process, which makes it difficult for the lubricant to form a lubricating film uniformly covering the contact surface in a short time, resulting in wear on the surface of the material, as depicted in Fig. S4 in the ESM.

In summary, when the SPAN65 content reaches 30 wt%, the wear resistance is the best. Therefore, a lubricant with an SPAN65 content of 30 wt% was selected for follow-up tests.

3.4 Effects of load and frequency on lubrication performance

The influences of the load and sliding frequency on the antiwear performance of PAO10/SP65 are analyzed. Figure 5(a) clearly shows that the COF ranges between 0.03 and 0.05 as the load varies from 1 to 5 N. When the loads are 10 and 20 N, the COF increases to 0.06–0.09. The wear area was analyzed with a 3D profiler. Figure 5(b) shows that when the load changes from 1 to 5 N, the wear correspondingly increases from 2,200 to 4,000 μm^3. At loads of 10 and 20 N, the wear increases to 7,800–12,000 μm^3. This may be because the lubrication film is easily damaged at

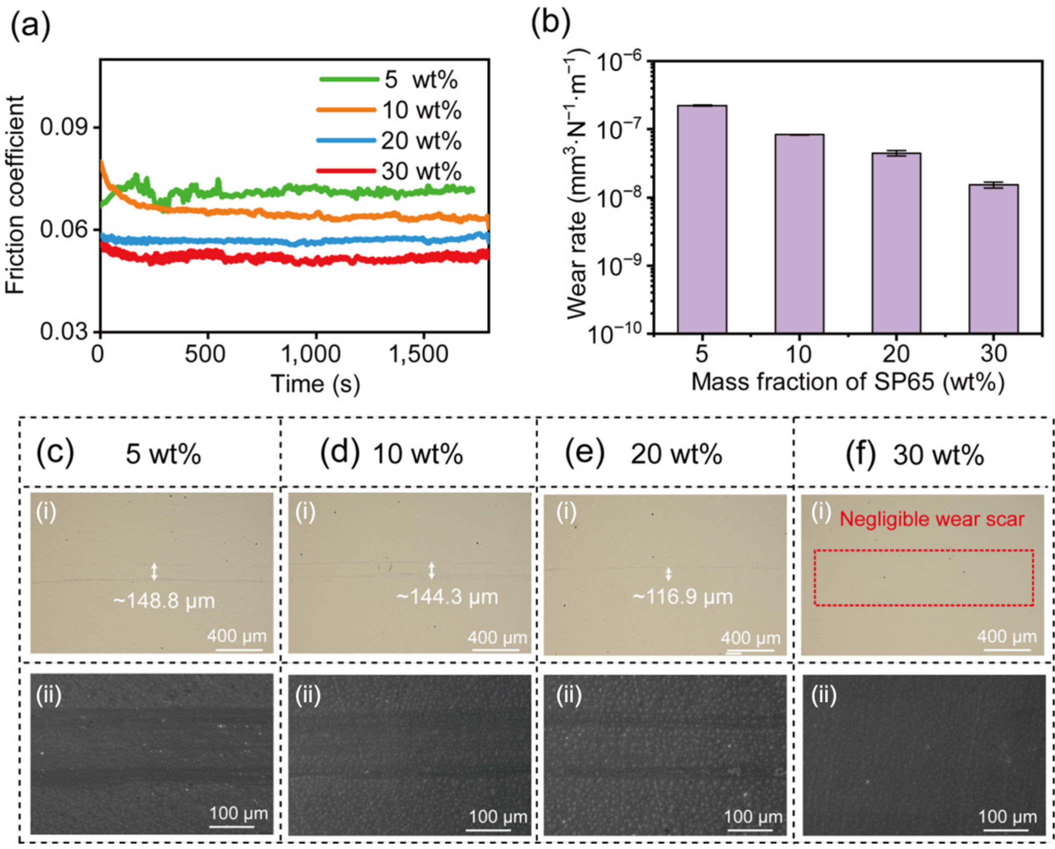

Fig. 4 (a) Friction coefficients of different mass fractions of PAO10/SP65. (b) Wear rates with different SPAN65 contents. (c–f) Wear marks of PAO10/SP65 lubricating friction pairs with different SPAN65 contents: (i) optical photographs and (ii) SEM images. The test load was 5 N, the frequency was 4 Hz, and the test time was 1,800 s.

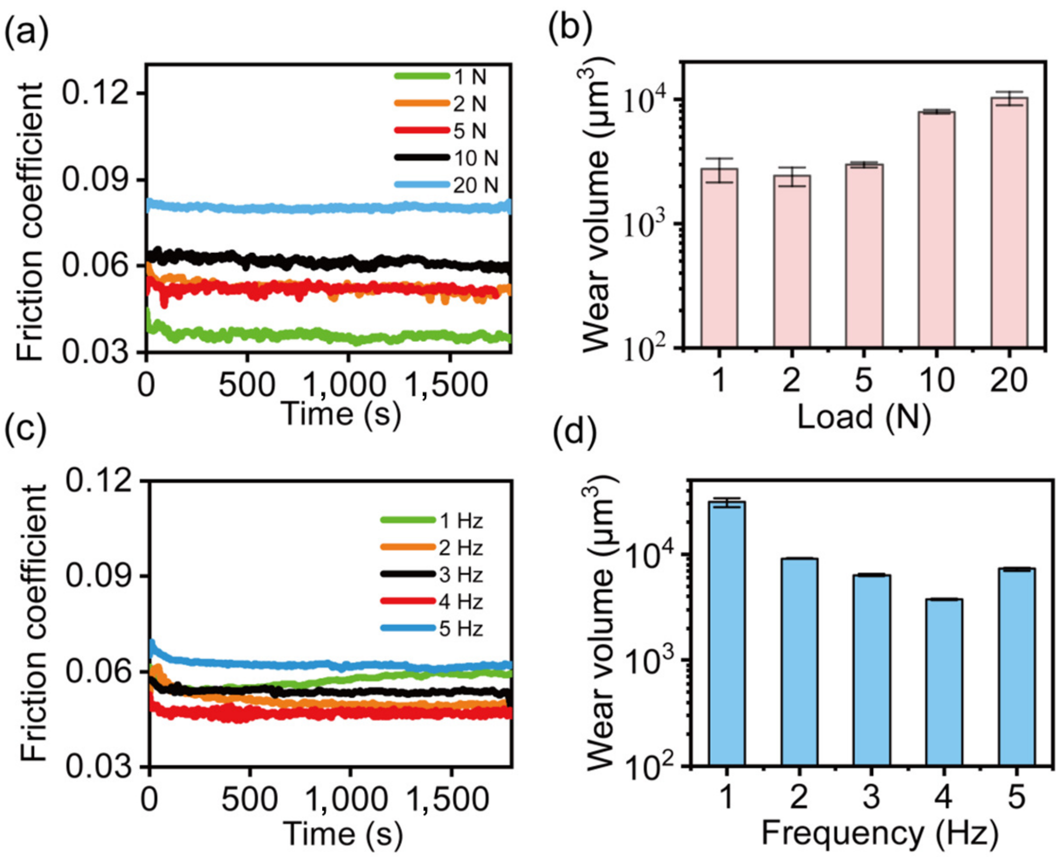

Fig. 5 (a) Friction coefficient of the PAO10/SP65 lubricant under loads ranging from 1 to 20 N, with 4 Hz as the sliding frequency. (b) Wear volume of the steel block under different loads; the frequency is 4 Hz. (c) Friction coefficient of PAO10/SP65 at frequencies ranging from 1 to 5 Hz, with 5 N as the load. (d) Wear volume of the steel block under various frequencies, and the load is 5 N.

higher pressures, which results in direct contact between the steel and steel surfaces, leading to an increased COF and a heightened degree of wear. Moreover, at low loads, the shear-thinning effect of PAO10/SP65 effectively reduced the viscous resistance of the friction process, and the lubricating film more evenly covered the surface of the two friction pairs, thus effectively reducing the contact between the friction pairs. At higher loads, although the shear-thinning effect of the lubricant can reduce the viscous resistance generated during friction, the thickness of the lubrication film may be reduced during this process so that the contact area between the two friction pairs becomes larger, resulting in increased surface wear and friction [35]. The wear area of the steel block was analyzed via optical microscopy. When the load is 1–5 N, the wear of the steel block can be negligible. When subjected to loads of 10 and 20 N, the steel block appeared to have noticeable scratches, as shown in Fig. S5 in the ESM.

As illustrated in Fig. 5(c), the COF is approximately 0.05 at frequencies of 1–4 Hz. At 5 Hz, the COF increases to approximately 0.07. The wear area was analyzed with a 3D profiler. As demonstrated in Fig. 5(d), the wear volumes of the steel surface at frequencies of 1 and 2 Hz are approximately 33,000 and 9,000 μm^3, respectively. This may be because the semisolid lubricant takes a long time to transform into fluid lubrication at a lower speed, resulting in the lubrication film formed during its friction process not being evenly distributed at the contact interface, so that the steel-steel interface is in direct contact, resulting in surface wear. At frequencies of 3 and 4 Hz, the wear volume is approximately 6,500 and 3,600 μm^3, respectively. This is because the appropriate frequency can facilitate the development of the lubricating film, thereby enhancing the antiwear performance of PAO10/SP65 [36]. At 5 Hz, the wear volume increases to approximately 7,600 μm^3. At higher speeds, the lubrication film may be destroyed due to the increase in shear stress, which reduces the lubrication effect and leads to increased wear. Moreover, the intermolecular force of PAO10/SP65 is weakened by the enhanced shear forces, resulting in a decreased lubricant viscosity and a reduced lubrication film thickness.

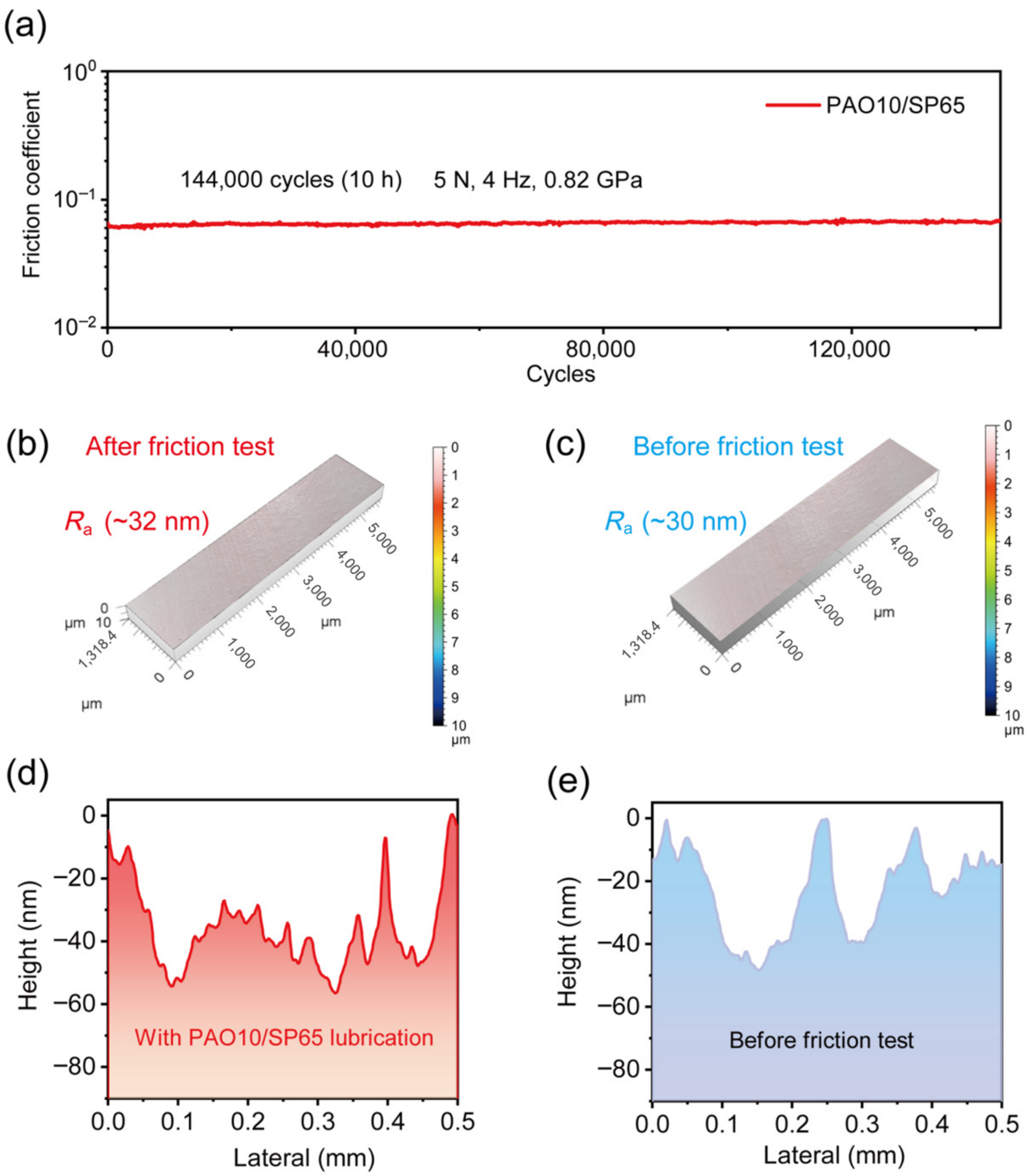

Fig. 6 (a) Friction coefficient of PAO10/SP65 after 10 h of friction testing. (b, c) 3D outline. (d, e) Depth of the wear area. The test load was 5 N and the frequency was 4 Hz.

In addition, the wear area was analyzed via optical microscopy. As illustrated in Fig. S6 in the ESM, at frequencies of 1 and 2 Hz, there are obvious wear marks on the steel block. At frequencies of 3 and 4 Hz, wear is negligible. At a frequency of 5 Hz, the steel block experiences slight wear. The experimental findings indicate that frequencies of 3 and 4 Hz are optimal for attaining ultra-low wear at the steel–steel interface in PAO10/SP65. Therefore, a load of 5 N and a frequency of 4 Hz were selected as the conditions for subsequent experiments.

3.5 Stability of the PAO10/SP65 ultra-low wear behavior

The stability of lubricants is the key factor in evaluating their lubrication performance. Therefore, the friction properties of the lubricant under different numbers of cycles were tested (Fig. 6 and Figs. S7 and S8 in the ESM). As shown in Fig. 6(a), after a 10 h friction experiment, the COF of PAO10/SP65 was approximately 0.05, and the friction curve was stable with almost no fluctuation. The wear area before and after the friction experiment was analyzed via a 3D profiler. As shown in Fig. 6(b), the 3D profile of the PAO10/SP65 lubricating steel block is almost free of wear and basically the same as that before friction after 10 hours of friction testing (Fig. 6(c)). In addition, the depth of the wear area barely changed before and after the experiment and was approximately 50 nm, as shown in Figs. 6(d) and 6(e). The experimental results show that PAO10/SP65 can achieve ultra-low wear at the steel–steel friction interface for a long period of time.

In addition, the wear rate and surface roughness at the wear area were measured before and after the experiment via a 3D profiler. The results indicate that following a 10-h friction test, the wear rate was determined to be 4.13×10^{-9} $mm^3\cdot N^{-1}\cdot m^{-1}$. The surface roughness of the steel block before and after the friction test was approximately 30 nm, with almost no difference, as shown in Fig. S9 in the ESM.

3.6 PAO10/SP65 achieves an ultra-low wear lubrication mechanism

To determine why PAO10/SP65 achieves ultra-low wear, the rheological properties of the lubricant were tested. At 25 °C and a frequency of 1 Hz and before the yield point (10 Pa), the loss modulus (G'') of PAO10/SP65 is considerably lower than the storage modulus (G'), indicating that the elasticity of PAO10/SP65 is greater than the viscosity, which directly proves that PAO10/SP65 exists in a semisolid form, as shown in Fig. 7(a). The trends of G' and G'' of the lubricating oil as a function of the shear frequency (from 0.1 to 100 Hz) were investigated under a shear stress of 5 Pa (Fig. 7(b)). G' is always greater than G'' throughout the test process, which indicates that PAO10/SP65 has good tolerance. Figure 7(c) clearly shows that PAO10/SP65 has shear-thinning properties. This shear-thinning property helps to reduce the viscous resistance during friction, thereby reducing friction and energy loss. As shown in Fig. 7(d), PAO10/SP65 demonstrated good creep recovery performance. Specifically, at elevated shear rates, the viscosity decreases. Conversely, at lower shear rates, the viscosity quickly reverts to its initial state. In addition, the Fe 2p spectra of the steel balls without friction and after the 10 h friction test revealed that no tribochemical reactions occurred during friction, as shown in Fig. S10 in the ESM. Furthermore, the anti-wear effect of this lubricant under high-load

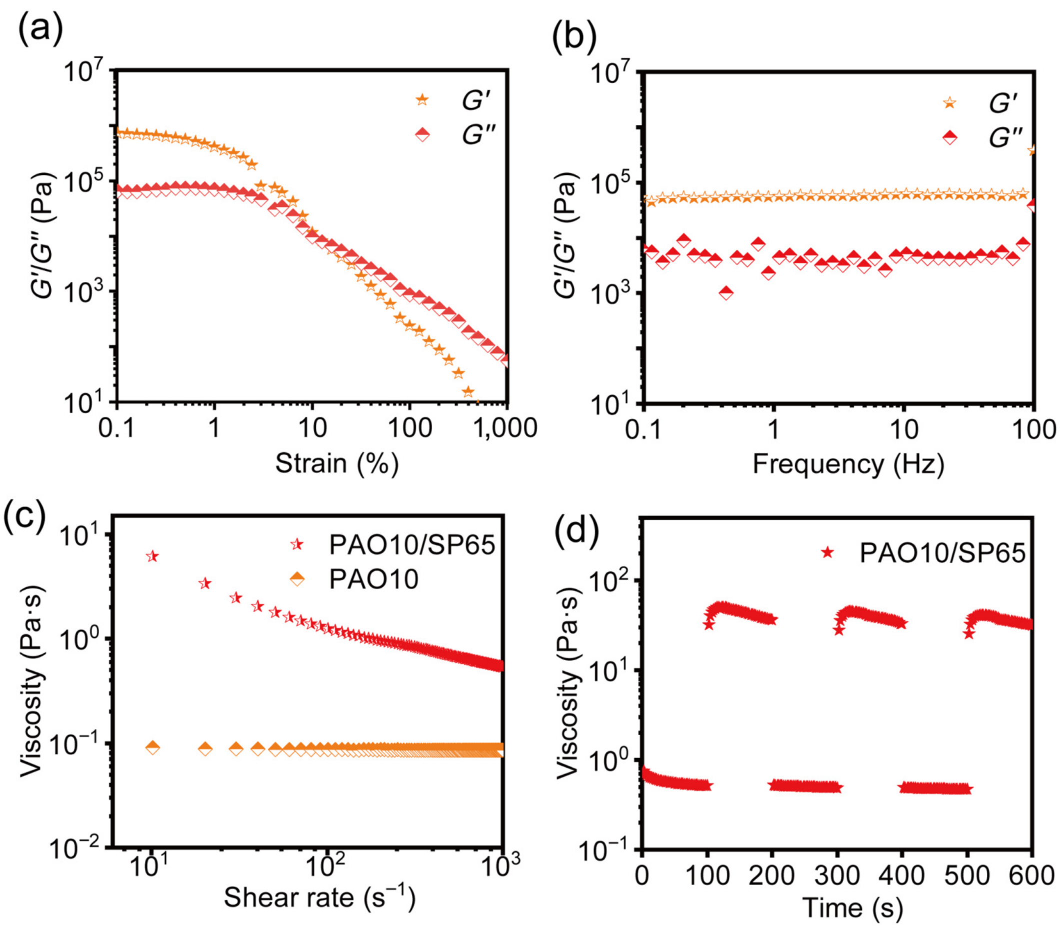

Fig. 7 Rheological properties of PAO10/SP65. (a) Relationship curve between G' and G'' with shear stress at a frequency of 1 Hz. (b) Relationships between G' and G'' as a function of shear frequency under a shear stress of 5 Pa. (c) Curve of viscosity with shear rate. (d) Viscosity curves at shear rates of 1,000 and 1 s^{-1}.

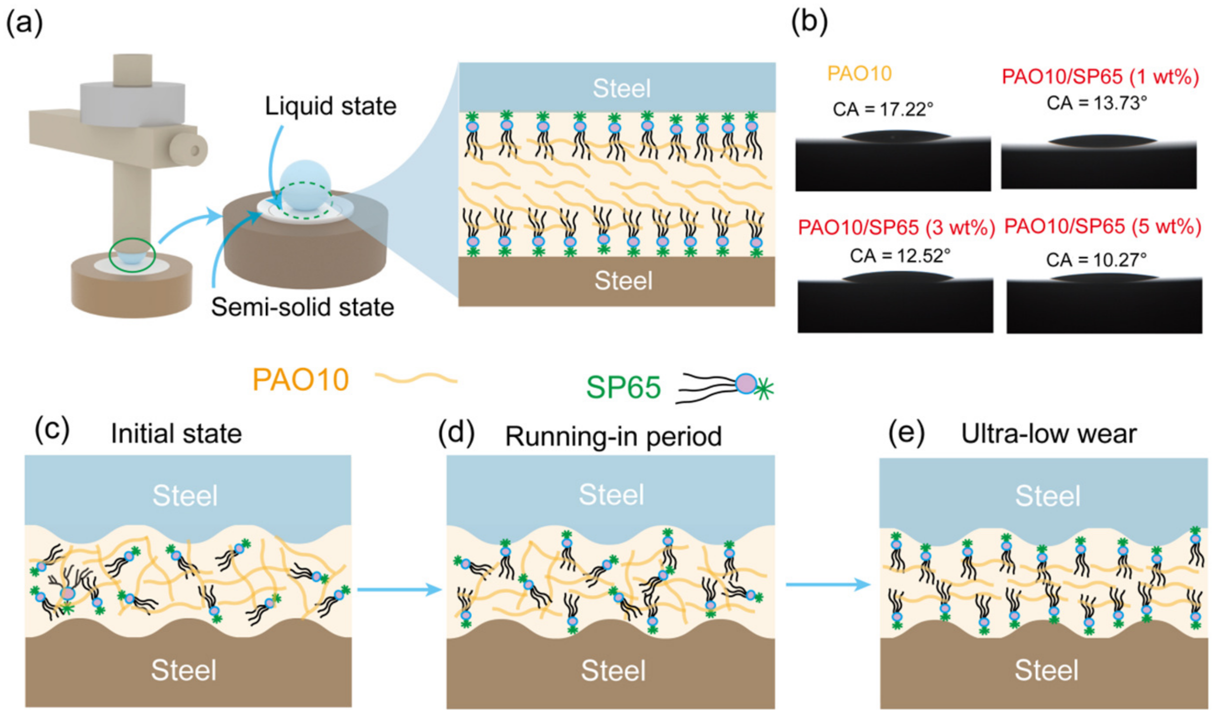

Fig. 8 (a) PAO10/SP65 lubrication mechanism diagram. (b) Contact angles of PAO10 and PAO10/SP65 (1, 3, and 5 wt%) on the steel block. (c) The initial phase, (d) the run-in phase, and (e) achieving ultra-low wear.

conditions is closely related to the formation and function of the Fe-O film, and it also exhibits excellent anti-wear performance in various friction pairs and lubricating oil systems (Figs. S11–S14 in the ESM).

After the above analysis, a lubrication model of PAO10/SP65 that may achieve ultra-low wear of steel to steel is proposed, as shown in Fig. 8. The reason why PAO10/SP65 achieves ultra-low wear at the steel–steel interface is mainly related to three factors. First, the presence of the hydroxyl group in SPAN65 enhances the adsorbability of the lubricant to the steel matrix, which enables the lubrication film formed by the lubricant during friction to be stably adsorbed onto the steel surface. As shown in Fig. 8(b), the measured contact angle SP65 of PAO10/SP65 at low concentrations at the steel surface is lower than that of PAO10, indicating good absorption of the lubricant at the steel surface. Second, the viscosity of PAO10/SP65 is reduced during friction, and this shear-thinning and viscosity–temperature property can reduce the viscous resistance during friction, thus reducing wear (Fig. 7(c), Figs. S15 and S16 in the ESM). Finally, the lubricant has good creep recovery ability (Fig. 7(d)), which means that during friction, the lubricant is semisolid at the periphery of the friction area and liquid in the friction area, resulting in a basin-like structure, which enables continuous and effective lubrication in the contact area. Figures 8(c)–8(e) show the three lubrication stages of the lubricant. Compared with the initial state, SAPN65 is rapidly adsorbed to the contact surface during the run-in stage, effectively reducing the contact between the steel and steel interfaces. Finally, a stable adsorption layer is formed so that the two contact surfaces can hardly contact each other directly.

4 Conclusions

The composite semisolid lubricant (PAO10/SP65) prepared in this work can achieve ultra-low wear of the steel–steel friction interface for a long time under a contact pressure of 0.82 GPa. This occurred because the addition of SPAN65 improved the adhesion of the lubricant to the steel surface and the bearing ability of the lubricating film formed during friction. Furthermore, the lubricant exhibited shear-thinning properties and good creep recovery ability, which helped reduce the viscous resistance during friction and maintain long-term adaptive lubrication performance. This study has enriched the lubrication material system for realizing ultra-low wear at the steel–steel friction interface and provided a new antiwear strategy for engineering steel.

Acknowledgements

We are grateful for the financial support of the Key Research Program of the Chinese Academy of Sciences (No. ZDBS-ZRKJZ-TLC010), the National Natural Science Foundation of China (Nos. 52205233, U21A2046, 52205230, and 52305233), the Strategic Priority Research Program of the Chinese Academy of Sciences (No. XDB 0470103), the Program for Taishan Scholars of Shandong Province (No. ts20190965), the Western Light Project of CAS (No. xbzg-zdsys-202118), the Major Science and Technology Projects in Gansu Province (No. 22ZD6GA002), the Major Program of the Lanzhou Institute of Chemical Physics CAS (No. ZYFZFX-5), the Natural Science Foundation of Gansu Province (No. 23JRRA610), the Natural Science Foundation of Shandong Province (No. ZR2024QE264), and the Key Research and Development Program in Shandong Province (No. SYS202203).

Declaration of competing interest

The authors have no competing interests to declare that are relevant to the content of this article. The author Daoai Wang is a Youth Editorial Board member of this journal.

Electronic Supplementary Material

Supplementary material is available in the online version of this article at https://doi.org/10.26599/FRICT.2025.9441070.

References

[1] Holmberg K, Erdemir A. Influence of tribology on global energy consumption, costs and emissions. *Friction* **5**(3): 263–284 (2017)

[2] Pasha M, Kaleemulla M. Erosive wear behavior of sprayed metal matrix composites: An overview. *P I Mech Eng J-J Eng* **227**(10): 1063–1075 (2013)

[3] Sun Y X, Song C F, Liu Z L, Li J W, Wang L, Sun C, Zhang Y Z. Tribological and conductive behavior of Cu/Cu rolling current-carrying pairs in a water environment. *Tribol Int* **143**: 106055 (2020)

[4] Liu X, Zhang J J, Zhang L Q, Feng Y G, Feng M, Luo N, Wang D A. Influence of interface liquid lubrication on triboelectrification of point contact friction pair. *Tribol Int* **165**: 107323 (2022)

[5] Xu Z C, Chau S N, Chen X Z, Zhang J, Li Y J, Dietz T, Wang J Y, Winkler J A, Fan F, Huang B R, et al. Assessing progress towards sustainable development over space and time. *Nature* **577**(7788): 74–78 (2020)

[6] Wang L C, Zhang L Q, Du C H, Yu T T, Feng M, Zhang X, Bu W F, Wang D A, Zhou F. Improved friction reduction and wear resistance of steel using a subnanometer nanowires-poly-α-olefin gel lubricant. *ACS Nano* **18**(50): 34288–34298 (2024)

[7] Liu H C, Wang X Y, Yang T, Su H G, Wang X B, Zhang S M, Lou W J. Rheological behaviors and tribological properties of nano-silica grease: A study compared with lithium grease and polyurea grease. *Tribol Int* **186**: 108657 (2023)

[8] Pawar R V, Hulwan D B, Mandale M B. Recent advancements in synthesis, rheological characterization, and tribological performance of vegetable oil-based lubricants enhanced with nanoparticles for sustainable lubrication. *J Clean Prod* **378**: 134454 (2022)

[9] Cai M R, Yu Q L, Liu W M, Zhou F. Ionic liquid lubricants: When chemistry meets tribology. *Chem Soc Rev* **49**(21): 7753–7818 (2020)

[10] Geurds L, Xu Y, Stokes J R. Friction of lubricated hydrogels: Influence of load, speed and lubricant viscosity. *Biotribology* **25**: 100162 (2021)

[11] Zhao J, Sheng W, Li Z, Zhang H, Zhu R P. Effect of lubricant selection on the wear characteristics of spur gear under oil-air mixed lubrication. *Tribol Int* **167**: 107382 (2022)

[12] Huo L X, Guo J S, Hu H J, Zhang K F, Zhou H, Liu P. Graphene nanosheets as lubricant additives: Effects of nature and size on lubricating performance. *Langmuir* **38**(31): 9678–9685 (2022)

[13] Vaitkunaite G, Espejo C, Wang C, Thiébaut B, Charrin C, Neville A, Morina A. MoS_2 tribofilm distribution from low viscosity lubricants and its effect on friction. *Tribol Int* **151**: 106531 (2020)

[14] Li J, Chen D J, Zhang H, Jiang Z W, Sun K, Fan J W, Tang Y H. The tribological properties of nano-lubricants and their application on bearings: Recent research progress. *Int J Adv Manuf Technol* **134**(7): 3051–3082 (2024)

[15] Ali M K A, Hou X J. Exploring the lubrication mechanism of CeO_2 nanoparticles dispersed in engine oil by bis(2-ethylhexyl) phosphate as a novel antiwear additive. *Tribol Int* **165**: 107321 (2022)

[16] Zhang W L, Qi X W, Yang X, Dong Y, Fan B L, Liang L. Fabrication of high-stability Ni-PSF@PAO40 microcapsules and their lubricating properties in polyamide 6. *Friction* **10**(12): 1985–1999 (2022)

[17] Li J J, Zhang C H, Luo J B. Superlubricity behavior with phosphoric acid–water network induced by rubbing. *Langmuir* **27**(15): 9413–9417 (2011)

[18] Du C H, Yu T T, Zhang L Q, Shen R L, Wu Z S, Li X J, He X J, Feng Y G, Wang D A. Robust and universal macroscale superlubricity with natural phytic acid solutions. *Tribol Int* **183**: 108387 (2023)

[19] Li J J, Zhang C H, Luo J B. Superlubricity achieved with mixtures of polyhydroxy alcohols and acids. *Langmuir* **29**(17): 5239–5245 (2013)

[20] Ma Q, Wang S J, Dong G N. Macroscale liquid superlubricity achieved with mixtures of fructose and diols. *Wear* **484–485**: 204037 (2021)

[21] Ma Q, Yan C P, Yan R, Xu X, Wang H F. Towards direct superlubricity and superlow wear via amino modification of polyhydroxy alcohol solutions. *Friction* **12**(9): 1980–1990 (2024)

[22] Ge X Y, Li J J, Zhang C H, Wang Z N, Luo J B. Superlubricity of 1-ethyl-3-methylimidazolium trifluoromethanesulfonate ionic liquid induced by tribochemical reactions. *Langmuir* **34**(18): 5245–5252 (2018)

[23] Ge X Y, Li J J, Zhang C H, Liu Y H, Luo J B. Superlubricity and antiwear properties of in situ-formed ionic liquids at ceramic interfaces induced by tribochemical reactions. *ACS Appl Mater Inter* **11**(6): 6568–6574 (2019)

[24] Du C H, Yang T, Yu T T, Zhang L Q, Sui X D, Feng Y G, Wang X B, Wang D A. Accelerating macroscale superlubricity through carbon quantum dots on engineering steel surfaces. *Adv Funct Mate* **34**(9): 2310880 (2024)

[25] Yu H X, Chen H J, Zheng Z W, Qiao D, Feng D P, Gong Z B, Dong G J. Effect of functional groups on tribological properties of lubricants and mechanism investigation. *Friction* **11**(6): 911–926 (2023)

[26] Cheung C K, Shi B, Lau C S, Shum P W, Zhou Z F, Li K Y. Investigating the effect of surface coatings on the wear behaviour of the friction contact in ultrasonic motors. *P I Mech Eng J-J-Eng* **224**(9): 989–996 (2010)

[27] Zhu Y Y, Qu H J, Luo M, He C L, Qu J J. Dry friction and wear properties of several hard coating combinations. *Wear* **456–457**: 203352 (2020)

[28] Yuan S, Lin N M, Zeng Q F, Zhang H X, Wang Z X, Tian L H, Qin L, Wang Z H, Tang B, Wu Y C. Research status of dry friction behavior of metallic materials: A brief review. *Surf Rev Lett* **27**(12): 2030003 (2020)

[29] Markov D P. Adhesion at friction and wear. *Friction* **10**(11): 1859–1878 (2022)

[30] Morón R C, Hernández-Onofre I, Contla-Pacheco A D, Bravo-Bárcenas D, Campos-Silva I. Friction and reciprocating wear behavior of borided AISI H13 steel under dry and lubricated conditions. *J Mater Eng Perform* **29**(7): 4529–4540 (2020)

[31] Liang X L, Liu Z Q, Wang B, Wang C J, Cheung C F. Friction behaviors in the metal cutting process: State of the art and future perspectives. *Int J Extrem Manuf* **5**(1): 012002 (2023)

[32] Resendiz-Calderon C D, Farfan-Cabrera L I, Oseguera-Peña J E, Cázares-Ramírez I, Gallardo-Hernandez E A. Friction and wear of metals under micro-abrasion, wet and dry sliding conditions. *J Mater Eng Perform* **29**(9): 6228–6238 (2020)

[33] Li G A, Hao S J, Gao W L, Lu Z. The effect of applied load and rotation speed on wear characteristics of Al–Cu–Li alloy. *J Mater Eng Perform* **31**(7): 5875–5885 (2022)

[34] Li Y L, Schreiber P, Schneider J, Greiner C. Tribological mechanisms of slurry abrasive wear. *Friction* **11**(6): 1079–1093 (2023)

[35] Wang L C, Zhang L Q, Zheng R H, Du C H, Yu T T, Li K P, Bu W F, Wang D A. Macroscale superlubrication achieved with shear-thinning semisolid lubricants. *Adv Mater* **36**(52): 2412257 (2024)

[36] Han T Y, Yi S, Zhang C H, Li J J, Chen X C, Luo J B, Banquy X. Superlubrication obtained with mixtures of hydrated ions and polyethylene glycol solutions in the mixed and hydrodynamic lubrication regimes. *J Colloid Interf Sci* **579**: 479–488 (2020)

Kunpeng Li received his B.S. degree (2022) in mechanical manufacturing and automation from Shanxi Agricultural University, China. He is currently studying at Qingdao University of Technology. He has focused mainly on research on antiwear materials.

Liqiang Zhang received his Ph.D. degree in Lanzhou Institute of Chemical Physics (LICP), Chinese Academy of Sciences (CAS). He is currently a research assistant in the State Key Laboratory of Solid Lubrication, LICP, CAS. His research mainly focuses on ultra-low friction and wear design, space tribology, and interfacial charge transport mechanism.

Youqiang Wang received his Ph.D. degree from China University of Petroleum, China. From 2001 to 2003, he worked as a postdoc at the School of Mechanical Engineering, Tianjin University, China. He is currently a professor and deputy director at Qingdao University of Technology, China. His research interests include tribology and surface interface engineering and aluminum magnesium metal material treatment and processing.

Daoai Wang received his Ph.D. degree from Lanzhou Institute of Chemical Physics, Chinese Academy of Sciences, China. From 2009 to 2010, he worked as a postdoc at the Max Planck Institute of Microstructure Physics, Germany. From 2010 to 2013, he worked as a JSPS researcher at the University of Tokyo, Japan. He is currently a professor and deputy director at the State Key Laboratory of Solid Lubrication, Lanzhou Institute of Chemical Physics, Chinese Academy of Sciences, China. His research interests include ultralow friction and wear design, space tribology, triboelectrification, physics and chemistry in tribology.